1876 J. Med. Chem. 2010, 53, 1876–1880
DOI: 10.1021/jm901200t

Journal of Medicinal Chemistry
Brief Article

De Novo Design of a Picomolar Nonbasic 5-HT$_{1B}$ Receptor Antagonist

David A. Nugiel,[†] Jennifer R. Krumrine,*[,†] Daniel C. Hill,[†] James R. Damewood, Jr.,[†] Peter R. Bernstein,[†] Cynthia D. Sobotka-Briner,[§] JianWei Liu,[§] Anna Zacco,[§] and M. Edward Pierson[‡]

[†]*Department of CNS Chemistry,* [§]*Department of Neuroscience Biology, and* [‡]*Neuroscience Therapeutic Area, AstraZeneca Pharmaceuticals, 1800 Concord Pike, Wilmington, Delaware 19850*

Received August 11, 2009

We describe herein the discovery of novel, de novo designed, 5-HT$_{1B}$ receptor antagonists that lack a basic moiety and that provide improved hERG and in vitro phospholipidosis profiles. We used a known 5-HT$_{1B}$ antagonist template as our starting point and focused on replacing the piperazine moiety. Pyrazole-based ideas were designed and synthesized among a small library of piperazine replacements. To our knowledge, these are the first potent, nonbasic, functionally active antagonists of the 5-HT$_{1B}$ receptor.

Introduction

5-HT$_1$ is the largest subgroup of the 5-hydroxytryptamine (5-HT[a]) family of receptors.[1] There are five receptor subtypes (5-HT$_{1A}$, 5-HT$_{1B}$, 5-HT$_{1D}$, 5-HT$_{1E}$, and 5-HT$_{1F}$), all of which are G-protein-coupled seven transmembrane receptors.[2] The 5-HT$_{1B}$ receptor has been targeted for its potential in the treatment of depression, anxiety, and other serotonergic neurotransmission related psychiatric disorders. It has been suggested that antagonists of the terminal 5-HT$_1$ autoreceptors (5-HT$_{1B/1D}$) may effect immediate 5-HT release, thereby increasing 5-HT transmission at the synapses. It is believed that this may provide faster clinical antidepressant activity than currently available therapies.[3] Recent studies on 5-HT$_{1B}$ selective antagonists are beginning to substantiate this hypothesis.[4]

It is generally accepted that known 5-HT receptor agonists and antagonists bind protonated amino groups to the highly conserved aspartic acid on transmembrane helix 3 (TM3).[5] These compounds have a characteristic basic amine site (pK_a > 7.5) embedded in an overall lipophilic (log D > 2) molecule. It is well-known that aryl-containing lipophilic bases[6] have a propensity to bind to the human ether-a-go-go related gene (hERG) channel. In addition, such amphiphilic cations have been implicated in phospholipidosis.[7]

Results

We describe here a series of novel, de novo designed 5-HT$_{1B}$ receptor antagonists that lack a basic moiety. These compounds demonstrate subnanomolar potency, are selective for the 5-HT$_{1B}$ receptor, and are active in a pharmacodynamic model of 5-HT$_{1B}$ receptor function. To our knowledge, these are the first potent, nonbasic, functionally active antagonists of the 5-HT$_{1B}$ receptor. In addition, the hERG and phospholipidosis safety characteristics of this series are improved over the piperazine series, which was our starting point for design.

Substituted quinolones[8] and chromans[9] are known 5-HT$_{1B}$ antagonist templates. We used a chroman template as the starting point for our design efforts (**1a**, Figure 1),[10] as this core had demonstrated superior drug metabolism and pharmacokinetics (DMPK) properties compared to quinolones.[11] With a focus on replacing the basic piperazine moiety, a variety of ideas were generated and ranked using the de novo design tool NovoFLAP.[12] NovoFLAP is a unique, ligand based, computer aided design approach that generates medicinally relevant ideas starting from compounds known to be active at a biological target of interest. A pyrazole-based idea (**1b**, Figure 1) was found to be particularly interesting, especially in light of a known inhibitor-bound crystal structure of transforming growth factor β (TGF$_\beta$) kinase.[13] This crystal structure exemplified a hydrogen bond between an aspartic acid residue and the pyrazole ring of the inhibitor. Motivated by these findings, several pyrazole-based ideas were included in a small library of piperazine replacements we designed and synthesized. We pursued these initial pyrazoles using the quinolone core because it was more amenable to library synthesis. The library was generated using the chemistry shown in Scheme 1.

Michael addition of 2-bromo-5-methylaniline into diethylacetylene dicarboxylate gave adduct **2** in 95% yield. This precursor was cyclized to the quinolone **3** under thermal conditions in 65% yield. Transamidation using sodium bis(trimethylsilyl)amide gave the key intermediate **4** in 90% yield. Using a Suzuki-based boronic acid coupling strategy,[14] a 40-member library of piperazine replacements was generated as exemplified by the synthesis of **5**. The chemistry was designed so that the piperazine replacement was inserted at the last step, maximizing the library's diversity potential.

*To whom correspondence may be addressed. Phone: (+)1 302 885 4772. Fax: (+)1 302 886 5382. E-mail: Jennifer.Krumrine@AstraZeneca.com.

[a] Abbreviations: 5-HT, 5-hydroxytryptamine; DMPK, drug metabolism and pharmacokinetics; GTPγS, guanosine γ-thiophosphate; TBTU, *O*-(benzotriazol-1-yl)-*N*,*N*,*N*′,*N*′-tetramethyluronium tetrafluoroborate; SPA, scintillation proximity assay; CHO, Chinese hamster ovary; EDTA, ethylenediaminetetraacetic acid; TM3, transmembrane helix 3; hERG, human ether-a-go-go related gene; TGF$_\beta$, transforming growth factor β; P-gp, permeability glycoprotein; PDB, protein crystal structure database; SEM, standard error of the mean; DCM, dichloromethane; EtOAc, ethyl acetate; THF, tetrahydrofuran; DME, 1,2-dimethoxyethane; fcc, flash column chromatography.

 Published on Web 01/20/2010

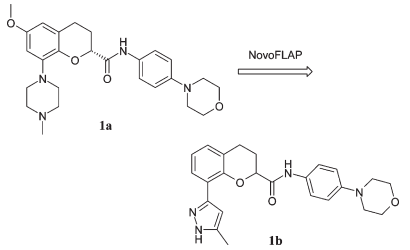

Figure 1. Initial de novo design of a pyrazole replacement for the piperazine ring in a 5-HT_{1B} antagonist using NovoFLAP.

Scheme 1[a]

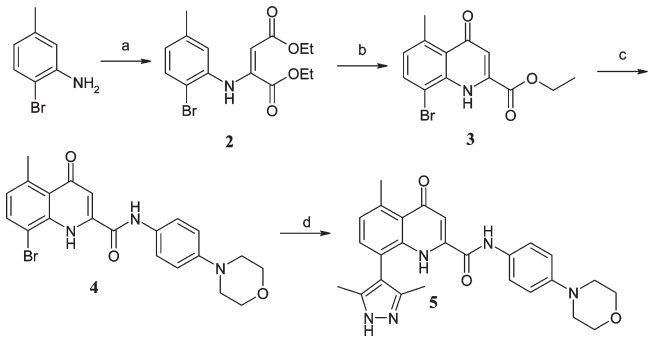

[a] Reagents: (a) diethylacetylene dicarboxylate, EtOH; (b) Dowtherm, 250 °C; (c) 4-morpholinoaniline, NaHMDS, THF; (d) boronic ester, $PdCl_2(PPh_3)_2$, K_2CO_3, 1:1 EtOH/water, 80 °C.

The library produced three hits having good binding affinity for the 5-HT_{1B} receptor, all of which contained pyrazole-based piperazine replacements. The most potent was **5** (Table 1) with a binding affinity of 9.3 nM (pK_i = 8.03). Unfortunately, functional activity evaluation of **5** revealed it to be a partial agonist (33% antagonist effect in a GTPγS binding assay). As we were interested in a compound having greater antagonist properties, we continued to optimize this initial promising lead. Our extensive experience with this class of 5-HT_{1B} templates allowed us to effectively incorporate the pyrazole-based piperazine replacement into a chroman-based template having all the physiochemical and DMPK properties needed for an in vivo tool compound. The chroman-based chemistry is detailed in Scheme 2. Subjecting ethyl 8-bromo-6-fluoro-4-oxo-4*H*-chromene-2-carboxylate[15] **6** to the same Suzuki reaction conditions shown in Scheme 1 gave the desired chromenone acid **7** in 58% yield. Compound **14** (Scheme 3) was coupled with chromenone **7** using TBTU in DMF to give the desired amide **8** in 85% yield.

Initial attempts to reduce chromenone **7** to chroman **9** using catalytic hydrogenation on a Parr apparatus only resulted in partial reduction at elevated temperature (70 °C) and pressure (80 psi). High pressure and temperature hydrogenation of chromenone **7** at 90 bar and 70 °C using an H-Cube[16] apparatus gave a nearly quantitative yield of hydroxyl chroman **9**. The hydroxyl group was then smoothly reduced using triethylsilane in trifluoroacetic acid at 80 °C to give the desired chroman **10** in 55% yield. Standard amide coupling conditions using TBTU in DMF gave the desired amide **11** in 65% yield.

Discussion

Table 1 shows the binding affinity and functional activity of the chroman-based analogues. The fully reduced chroman **11** was a potent compound with a binding affinity of 0.96 nM (pK_i = 9.02) but with a disappointing functional activity profile of a partial agonist (62% antagonist effect).[17] Fortunately, chromenone **8** had the desired functional activity profile. It had high affinity for the 5-HT_{1B} receptor (0.43 nM, pK_i = 9.37) and behaved as a full antagonist in our GTPγS binding assay (90% antagonist effect). In addition, the compound had moderate clearance and was a moderate permeability glycoprotein (P-gp) substrate.[18] **8** was evaluated at 10 μM in a broad selectivity screen of 100 targets (MDS Pharma) and was found to be inactive except at the 5-HT_{1B} receptor.[19] Shown in Table 2 is the selectivity profile of **8** versus several 5-HT receptor subtypes that are closely related to the 5-HT_{1B} receptor and were among the 100 targets in the MDS Pharma panel. These overall qualities were sufficient to examine the

Table 1. 5-HT_{1B} Receptor Binding Affinities and % Antagonist Effect on [^{35}S]GTPγS Binding in CHO Cells Expressing 5-HT_{1B} Receptors, and Selected Measured pK_a Values

compd	5-HT_{1B} K_i (nM) ($pK_i \pm$ SEM)	% antagonist effect ± SEM	pK_a base 1	pK_a base 2
AZD1134	1.7 (8.76 ± 0.055)	150 ± 13	7.3 ± 0.05	2.5 ± 0.05
1a	12 (7.91 ± 0.043)	120 ± 2.0	7.66 ± 0.05	
5	9.3 (8.03 ± 0.075)	33 ± 0.040		
8	0.43 (9.37 ± 0.23)	90 ± 1.6	2.87 ± 0.01	2.05 ± 0.01
11	0.96 (9.02 ± 0.52)	62 ± 7.1	3.28 ± 0.05	

Scheme 2[a]

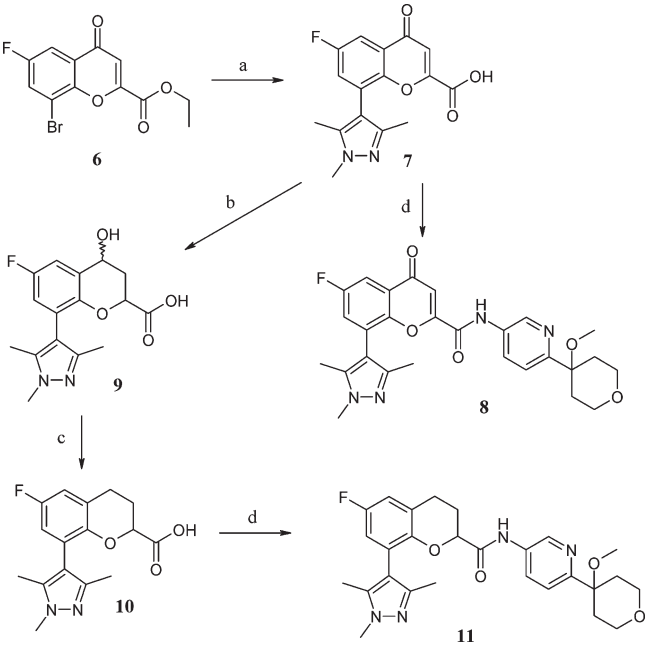

[a] Reagents: (a) $PdCl_2(PPh_3)_2$, K_2CO_3, pyrazole, DME/EtOH/water, 90 °C; (b) H_2, MeOH/HOAc/IPA, 90 bar, 70 °C; (c) Et_3SiH, TFA, 80 °C; (d) **14**, TBTU, DMF.

Scheme 3[a]

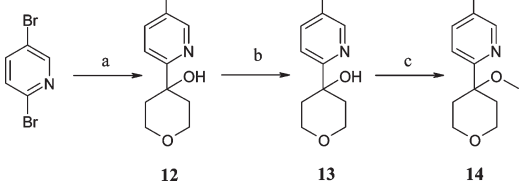

[a] Reagents: (a) *n*-BuLi, dihydro-2*H*-pyran-4(3*H*)-one, THF, −78 °C; (b) CuCl, Cu, 7 N NH_3 in MeOH, 100 °C; (c) MeOH, TFA, 80 °C.

Table 2. Selectivity Profile of **8** versus Several 5-HT Receptor Subtypes[a]

receptor	% effect at 10 μM	species
5-HT_{1A}	−8	human
5-HT_{2A}	−5	human
5-HT_{2B}	4	human
5-HT_4	30	guinea pig

[a] **8** was tested in several binding assays available through MDS Pharma for 5-HT receptors closely related to the 5-HT_{1B} receptor and found to be selective. Additional information on assay protocols and standards are available through MDS Pharma Services.[19]

compound's behavior in vivo. Therefore, **8** was evaluated in an agonist induced hypothermia model of central 5-HT_{1B} receptor function in the guinea pig.[20] Details of the protocol can be found in the Supporting Information. It has been demonstrated previously that 5-HT_{1B} receptors and not 5-HT_{1D} receptors mediate the hypothermic response in guinea pigs.[21] The results are shown in Figure 2. Here, **8** shows a dose dependent reversal of agonist-induced hypothermia while having no effect on body temperature when given alone, indicating its temperature modifying effect was mediated by a 5-HT_{1B} antagonist-based mechanism.

In addition to the desirable in vitro and in vivo activities described, pyrazoles generally had hERG IC_{50}[22] improved over the range typically observed among the piperazine analogues, (0.7 to >33 μM). For example, the hERG IC_{50} of piperazine **1a** was 19 μM (95% confidence interval, 15.6−24.7 μM) and 81% maximum observed effect at 100 μM. In comparison, most pyrazoles had IC_{50} > 33 μM, the upper limit of detection for our standard assay, and all had IC_{50} > 25 μM. For **8**, the hERG IC_{50} was 95 μM (extrapolated value due to precipitation at 100 μM, 95% confidence interval of 46.5−193 μM) with only a 26% maximum observed effect at 33 μM. Further, no pyrazole showed activity in our in vitro phospholipidosis assay,[23] an improvement over the piperazines. For piperazine **1a**, the maximum observed effect at 300 μM was 81%. For pyrazoles **5** and **8**, the maximum observed effect at 300 μM was 12% and 9%, respectively, where 20% is the threshold of detection for phospholipogenic activity. Compound **11** was not tested. In comparison, the piperazine analogues of **5** and **11** had maximum observed effects at 300 μM of 105% and 99%, respectively. The piperazine analogue of **8** was not tested.

Discussion and Conclusions

With the de novo design tool NovoFLAP, pyrazole replacements were identified for the ubiquitous piperazine moiety found in 5-HT_{1B} antagonists, which is believed to form a key interaction with an aspartic acid. Analysis of the protein crystal structure database (PDB) provided supporting evidence for a pyrazole ring having the capacity to hydrogen-bond with an aspartic acid residue in the required manner. A 40-membered scouting library was designed in which three pyrazole-containing analogues with excellent 5-HT_{1B} binding affinity were found. Further refinement led to compounds with subnanomolar affinity for the 5-HT_{1B} receptor and a range of in vitro functional activities from partial agonist to antagonist. Additionally, these same compounds exhibited acceptable DMPK properties, excellent profiles with respect to in vitro hERG and phospholipidosis assays, and potent 5-HT_{1B} antagonist activity in our guinea pig hypothermia pharmacodynamic model.

We have thus demonstrated, for the first time, that an amine that will be positively charged at physiological pH is not needed for in vitro and in vivo activity at the 5-HT_{1B} receptor.

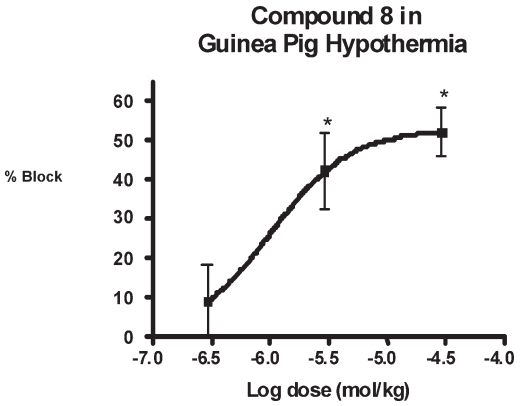

Figure 2. Dose dependent effect of **8** in an agonist induced guinea pig hypothermia model.

Experimental Section

Biological Assays. 1. 5-HT_{1B} Receptor Competition Binding Studies. Frozen membrane preparations of stably transfected Chinese hamster ovary (CHO) cells expressing 5-HT_{1B} receptors (Perkin-Elmer, 10 mg/mL) were rapidly thawed, briefly vortexed, and diluted in assay buffer (AB) containing 50 mM Tris-HCl, 4 mM $MgCl_2$, 4 mM $CaCl_2$, 1 mM EDTA, pH 7.4. Membranes were resuspended in AB at 125 μg/mL and dispensed at 80 μL per well for a final concentration of 10 μg/well. Assay plates are white, 96-well OptiPlates (PerkinElmer). Test compounds were solubilized in DMSO at 10 mM. For concentration response analyses, 11 serial dilutions (10 μM to 170 pM, final concentration) of compound were prepared in DMSO from 10 mM stock solutions. The stock radioligand was diluted in AB/0.1% ascorbic acid to 10× the concentration needed for the assay. AZD1134[24] (FW 521.6) was used to define nonspecific binding at a final assay concentration of 1 μM. Final assay volumes per well were 2 μL of compound/nonspecific, 80 μL membranes, 20 μL of [^{3}H]GR125743 (Amersham, TRK1046) at 0.5 nM final concentration. The assay plates were incubated for 1 h at room temperature with shaking. Yttrium silicate-WGA SPA beads (Amersham RPNQ0011 or RPNQ0023) were resuspended at 15 mg/mL in AB, and an amount of 100 μL was added for 1.5 mg/well final. Plates were incubated for an additional 30 min with high speed shaking to keep the beads in suspension. Then the plates were centrifuged and counted on the Top Count (PerkinElmer).

Data were analyzed by calculating IC_{50} and K_i using the Kenakin correction for ligand depletion (see equations below),

$$B = [(K_D + L_T + R_T) - \{(K_D + L_T + R_T)^2 - 4R_T L_T\}^{1/2}]/2$$

$$K_i = (0.5B)(IC_{50})(K_D)/[(L_T R_T) + 0.5B(R_T - L_T + 0.5B - K_D)]$$

where L_T and R_T are the total concentrations of the ligand and receptor, respectively (in nM).

2. GTPγ^{35}S Functional Antagonist Assay. Membranes and compound dilutions used for the GTPγS assay were the same as those in the 5-HT_{1B} receptor binding assay. In this scintillation proximity assay (SPA), membranes (15 mg of protein/well) and WGA PVT beads (50 mg/well) (Amersham RPNQ0001) were preincubated in bulk in assay buffer containing 20 mM HEPES, 100 mM NaCl, 10 mM $MgCl_2$, 0.1% BSA, pH 7.4, for 30 min. After addition of GTPγ^{35}S (200 pM final assay concentration) and GDP (10 mM final) to the membrane/bead mixture, 150 mL of the mixture was added to 96-well OptiPlates (PerkinElmer) containing 2 mL of compounds. After 5 min of preincubation, an amount of 50 mL of buffer or 108 nM 5-HT (27 nM final

assay concentration, EC_{80}) was added. The plates were incubated for 1 h with shaking and then counted in a TopCount (PerkinElmer).

Percent effect with respect to basal (buffer unstimulated) and stimulated (EC_{80} of 5-HT) response was determined. IC_{50} was defined as 50% inhibition of the stimulated response.

Chemistry. All commercially available reagents and solvents were used without further purification unless otherwise stated. Automated flash chromatography was performed on an ISCO CombiFlash using Biotage Flash cartridges with peak detection at 254 nm. ^{1}H NMR spectra were recorded on a Bruker Avance instrument operating at 300 or 500 MHz with tetramethylsilane or residual protonated solvent used as a reference. Low resolution mass spectra were recorded using a Waters Micromass ZQ quadrupole mass spectrometer linked to a Hewlett-Packard HP1100 LC system with UV detector at 254 nm. Sample injection is done by a Gilson 215 autosampler. The mobile phase consisted of a gradient using water with 0.1% formic acid and acetonitrile with 0.1% formic acid. The spectrometer has an electrospray source operating in positive and negative ion mode. Additional detection is achieved using a Sedex 55 ELS detector. All compounds were found to have a purity of >95% by this method. High-resolution mass spectra were recorded on an Agilent Technologies 6210 time-of-flight LC/MS spectrometer.

2: (*E*)-2-(2-Bromo-5-methylphenylamino)but-2-enedioic Acid Diethyl Ester. A solution of 2-bromo-5-methylphenylamine (1.4 g, 10.0 mmol) in ethanol (10 mL) was treated with diethylacetylene dicarboxylate (1.7 mL, 10.0 mmol) and heated to 60 °C for 2 h. The mixture was cooled and the solvent evaporated at reduced pressure. Chromatography (silica, 0−30% EtOAc/hexane) gave the product as an oil (3.4 g, 96%). LC/MS 2.96 min, m/z 356 (M + H); ^{1}H NMR (300 MHz, $CDCl_3$) δ 1.08 (t, 3H), 1.12 (t, 3H), 2.02 (s, 3H), 4.07 (q, 2H), 4.16 (q, 2H), 5.49 (s, 1H), 6.37 (m, 1H), 7.22 (m, 2H), 8.53 (bs, 1H).

3: 8-Bromo-5-methyl-4-oxo-1,4-dihydroquinoline-2-carboxylic Acid Ethyl Ester. A solution of (*E*)-2-(2-bromo-5-methylphenylamino)but-2-enedioic acid diethyl ester (3.4 g, 9.6 mmol) in Dowtherm (5 mL) was added dropwise to Dowtherm (30 mL) at 250 °C over 2 min. During the addition the internal temperature was kept above 240 °C. After 5 min the mixture was cooled to room temperature. The mixture was subjected directly to chromato graphy (silica, 0−70% EtOAc/hexane) to give the desired product as a solid (2.5 g, 84%). Mp 135 °C; LC/MS 2.40 min, m/z 310 (M + H); ^{1}H NMR (300 MHz, $CDCl_3$) δ 1.09 (t, 3H), 2.43 (s, 3H), 4.05 (q, 2H), 6.54 (s, 1H), 6.89 (m, 1H), 7.58 (m, 1H), 9.20 (bs, 1H).

4: 8-Bromo-5-methyl-4-oxo-1,4-dihydroquinoline-2-carboxylic Acid (4-Morpholin-4-ylphenyl)amide. A solution of 8-bromo-5-methyl-4-oxo-1,4-dihydroquinoline-2-carboxylic acid ethyl ester (4.6 g, 14.9 mmol) and 4-morpholin-4-ylphenylamine (2.65 g, 14.9 mmol) in THF (40 mL) was cooled to 0 °C. Sodium bis(trimethylsilyl)amide (45 mL, 45 mmol) was added dropwise over 2 min. The mixture was stirred at 0 °C for 1 h, then poured into water and extracted with DCM. The organic layer was separated and dried ($MgSO_4$) and the solvent removed at reduced pressure. The product was recrystallized from acetonitrile to give a yellow solid (5.0 g, 76%). Mp 144 °C; LC/MS 2.54 min, m/z 442 (M + H); ^{1}H NMR (300 MHz, $CDCl_3$) δ 2.41 (s, 3H), 2.58 (m, 4H), 3.72 (m, 4H), 6.70 (m, 2H), 6.91 (m, 2H), 7.61 (m, 1H), 7.74 (m, 2H), 9.11 (bs, 1H), 9.84 (bs, 1H).

5: 5-Methyl-4-oxo-8-(1*H*-pyrazol-4-yl)-1,4-dihydroquinoline-2-carboxylic Acid (4-Morpholin-4-yl-phenyl)amide. A suspension of 8-bromo-5-methyl-4-oxo-1,4-dihydroquinoline-2-carboxylic acid (4-morpholin-4-ylphenyl)amide (1.5 g, 4.59 mmol), 4-(4,4,5,5-tetramethyl-1,3,2-dioxaborolan-2-yl)-1*H*-pyrazole (1.6 g, 6.88 mmol), and potassium carbonate (1.9 g, 13.76 mmol) in a 7:3:2 THF/EtOH/water mixture (70 mL) was treated with bis(triphenylphosphine)palladium(II) dichloride (0.322 g, 0.46 mmol) and heated to 100 °C for 3 h. The mixture was cooled, diluted with water, extracted with DCM and the organic layer separated, dried ($MgSO_4$), and concentrated. The product was isolated by preparative HPLC to give the desired product as a solid (83 mg, 5%). Mp 153 °C; LC/MS 2.30 min, m/z 430 (M + H); ^{1}H NMR (300 MHz, $CDCl_3$) δ 2.39 (s, 3H), 2.58 (m, 4H), 3.72 (m, 4H), 6.70 (m, 3H), 6.88 (m, 1H), 7.07 (m, 1H), 7.74 (m, 2H), 8.15 (m, 2H), 8.89 (bs, 1H), 9.11 (bs, 1H), 9.84 (bs, 1H). HRMS: calcd M + H = 430.4906, found M + H = 430.4922.

7: Potassium 6-Fluoro-4-oxo-8-(1,3,5-trimethyl-1*H*-pyrazol-4-yl)-4*H*-chromene-2-carboxylate. A slurry of ethyl 8-bromo-6-fluoro-4-oxo-4*H*-chromene-2-carboxylate (1.24 g, 3.93 mmol), 1,3,5-trimethyl-4-(4,4,5,5-tetramethyl-1,3,2-dioxaborolan-2-yl)-1*H*-pyrazole (1.23 g, 5.21 mmol), bis(triphenylphosphine)-palladium(II) chloride (276 mg, 0.39 mmol), potassium carbonate (1.63 g, 11.8 mmol), DME (50 mL), water (21 mL), and ethanol (14 mL) was vacuum degassed (three cycles) and then heated to 90 °C for 16 h. Reaction was cooled to room temperature and filtered through Celite. Solids were washed with DME (3 × 20 mL), and filtrate was evaporated. DME was added (30 mL) and evaporated (3×) to azeotrope water. This solid was suspended in 50 mL of DME, filtered, washed with more DME, and dried under high vacuum for 3 h. The pink crude solid potassium salt was typically carried on in further reactions without purification (0.66 g, 58%). LC/MS 0.82 min, m/z 317 (M + H); ^{1}H NMR (300 MHz, DMSO-d_6) δ ppm 2.13 (s, 3 H), 2.23 (s, 3 H), 3.74 (s, 3 H), 6.68 (s, 1 H), 7.51 (dd, J = 9.0, 2.8 Hz, 1 H), 7.57−7.77 (m, 1 H).

8: 6-Fluoro-*N*-(6-(4-methoxytetrahydro-2*H*-pyran-4-yl)pyridin-3-yl)-4-oxo-8-(1,3,5-trimethyl-1*H*-pyrazol-4-yl)-4*H*-chromene-2-carboxamide. To a solution of potassium 6-fluoro-4-oxo-8-(1,3,5-trimethyl-1*H*-pyrazol-4-yl)-4*H*-chromene-2-carboxylate (240 mg, 0.68 mmol) in DMF (3 mL) was added 6-(4-methoxytetrahydro-2*H*-pyran-4-yl)pyridin-3-amine (111 mg, 0.53 mmol), and Hunig's base (200 μL, 1.15 mmol). When all had dissolved, 2-(1*H*-benzo[*d*][1,2,3]triazol-1-yl)-1,1,3,3-tetramethylisouronium tetrafluoroborate (340 mg, 1.06 mmol) was added all in one portion and the mixture was stirred for 1 h. DMF was evaporated. Residue was mixed with EtOAc (30 mL) and extracted with 20% K_2CO_3 (2 × 10 mL), then brine. Organic layer was dried over Na_2SO_4, filtered, and evaporated to give an oil which was purified by fcc on silica (12 g) DCM to 10% MeOH in DCM. This gave a light-yellow solid (230 mg, 85%). Mp 132−134 °C LC/MS 2.22 min, m/z 507 (M + H); ^{1}H NMR (500 MHz, $CDCl_3$) δ ppm 1.57 (br. s., 3 H), 1.95 (d, J = 13.1 Hz, 2 H), 2.06 - 2.42 (m, 6 H), 2.80 (s, 3 H), 2.96−3.16 (m, 3 H), 3.68−4.07 (m, 4 H), 7.34 (dd, J = 7.9, 3.1 Hz, 1 H), 7.54 (d, J = 8.5 Hz, 1 H), 7.87 (dd, J = 7.8, 3.2 Hz, 1 H), 8.10−8.34 (m, 2 H), 8.59 (d, J = 2.4 Hz, 1 H). HRMS: calcd M + H = 507.2038 found M + H = 507.2061.

9: 6-Fluoro-4-hydroxy-8-(1,3,5-trimethyl-1*H*-pyrazol-4-yl)chroman-2-carboxylic Acid. A solution of potassium 6-fluoro-4-oxo-8-(1,3,5-trimethyl-1*H*-pyrazol-4-yl)-4*H*-chromene-2-carboxylate (780 mg, 2.47 mmol) in MeOH (100 mL)/acetic acid (40 mL)/IPA (60 mL) was pumped through the H-Cube using 10% Pd/C catalyst (medium CatCart part no. THS 01121, 1 mL/min, 90 barr of H_2, 70 °C, hydrogen controlled). Eluate was evaporated under reduced pressure and residue was purified by fcc on silica (12 g) DCM to 20% MeOH in DCM to give a white solid (750 mg, 95%). LC/MS 0.75 min, m/z 321 (M + H); ^{1}H NMR (500 MHz, MeOD) δ ppm 2.10 (s, 3 H), 2.15 (s, 3 H), 2.45−2.53 (m, 1 H), 3.71 (s, 3 H), 4.54−4.62 (m, 1 H), 4.92 (dd, J = 8.7, 6.3 Hz, 1 H), 6.74 (dd, J = 8.9, 3.1 Hz, 1 H), 7.12 (dd, J = 9.0, 3.2 Hz, 1 H).

10: 6-Fluoro-8-(1,3,5-trimethyl-1*H*-pyrazol-4-yl)chroman-2-carboxylic Acid. To a flask containing 6-fluoro-4-hydroxy-8-(1,3,5-trimethyl-1*H*-pyrazol-4-yl)chroman-2-carboxylic acid (750 mg, 2.34 mmol) was added triethylsilane (10 mL, 62.61 mmol) followed by trifluoroacetic acid (5 mL, 64.90 mmol). The mixture was heated to 90 °C for 3 h. Excess reagents were evaporated under reduced pressure. Residue was dissolved in 20 mL of 3 N HCl and extracted with $CHCl_3$ (4 × 20 mL). Organic layers were dried over Na_2SO_4, filtered, and evaporated. Crude product was purified by fcc on silica (4 g) DCM to 10% MeOH/DCM to give 6-fluoro-8-(1,3,5-trimethyl-1*H*-pyrazol-4-yl)chroman-2-carboxylic acid (392 mg, 55.0%). LC/MS

2.00 min, m/z 305 (M + H); ^{1}H NMR (500 MHz, $CDCl_3$) δ ppm 2.00−2.47 (m, 8 H), 2.74−3.08 (m, 2 H), 3.74−4.10 (m, 3 H), 4.65 (dd, J = 7.5, 3.5 Hz, 1 H), 5.55 (br s, 1 H), 6.66 (dd, J = 8.5, 3.1 Hz, 1 H), 6.82 (dd, J = 8.4, 2.9 Hz, 1 H).

11: 6-Fluoro-*N*-(6-(4-methoxytetrahydro-2*H*-pyran-4-yl)pyridin-3-yl)-8-(1,3,5-trimethyl-1*H*-pyrazol-4-yl)chroman-2-carboxamide. To a solution of 6-fluoro-8-(1,3,5-trimethyl-1*H*-pyrazol-4-yl)chroman-2-carboxylic acid (33 mg, 0.11 mmol) and 6-(4-methoxytetrahydro-2*H*-pyran-4-yl)pyridin-3-amine (22.6 mg, 0.11 mmol) in DMF (3 mL) containing Hunig's base (70 μL, 0.40 mmol was added 2-(1*H*-benzo[*d*][1,2,3]triazol-1-yl)-1,1,3,3-tetramethylisouronium tetrafluoroborate (52.2 mg, 0.16 mmol). The mixture was stirred for 1 h, and then additional 2-(1*H*-benzo[*d*][1,2,3]triazol-1-yl)-1,1,3,3-tetramethylisouronium tetrafluoroborate (52.2 mg, 0.16 mmol) was added. The mixture was stirrred for an additional 1 h. DMF was evaporated, residue was mixed with 20 mL of EtOAc and extracted with 20% K_2CO_3 (3 × 10 mL), then brine (10 mL). Organic layer was dried over Na_2SO_4, filtered, and evaporated. Product was purified by fcc on silica (4 g) DCM to 10% MeOH/DCM to give 6-fluoro-*N*-(6-(4-methoxytetrahydro-2*H*-pyran-4-yl)pyridin-3-yl)-8-(1,3,5-trimethyl-1*H*-pyrazol-4-yl)chroman-2-carboxamide (35.0 mg, 65.3%). LC/MS 2.29 min, m/z 495 (M + H); ^{1}H NMR (300 MHz, $CDCl_3$) δ ppm 0.62−1.48 (m, 2 H), 1.66 (br s, 1 H), 1.83−2.47 (m, 10 H), 2.47−2.79 (m, 1 H), 2.78−3.25 (m, 4 H), 3.56−4.10 (m, 6 H), 4.59 (d, J = 10.3 Hz, 1 H), 6.59−6.99 (m, 2 H), 7.45 (d, J = 8.6 Hz, 1 H), 7.89−8.24 (m, 2 H), 8.30−8.79 (m, 1 H). HRMS: calcd M + H = 495.2402, found M + H = 495.2400.

Acknowledgment. The authors thank Jim Hall for providing NMR support, Timothy Blake for MS support, Christopher Holmquist for the initial library synthesis, Paul Warwick for synthesis of intermediates, Paul Ciaccio for evaluating the phospholipogenic potential, and Herbert Barthlow and Matthew Bridgland-Taylor for evaluating the hERG potential.

Supporting Information Available: Preparation details of **14**, described in Scheme 3, preparative reverse phase chromatography, guinea pig hypothermia assay protocol. This material is available free of charge via the Internet at http://pubs.acs.org.

References

(1) Hoyer, D.; Hannon, J. P.; Martin, G. R. Molecular, pharmacological and functional diversity of 5-HT receptors. *Pharmacol., Biochem. Behav.* **2002**, *71*, 533–554.
(2) Hartig, P. R.; Hoyer, D.; Humphrey, P. P.; Martin, G. R. Alignment of receptor nomenclature with the human genome: classification of 5-HT_{1B} and 5-HT_{1D} receptor subtypes. *Trends Pharmacol. Sci.* **1996**, *17*, 103–105.
(3) Slassi, A. Recent advances in 5-$HT_{1B/1D}$ receptor antagonists and agonists and their potential therapeutic applications. *Curr. Top. Med. Chem.* **2002**, *2*, 559–574.
(4) Helal, C. J. Potent and Selective 5-HT1B/D Antagonists/Inverse Agonists with Reduced hERG Affinity for the Treatment of Depression. Presented at the 235th National Meeting of the American Chemical Society, New Orleans, LA, Apr 6−10, **2008**; MEDI-154.
(5) Trumpp-Kallmeyer, S.; Hoklack, J.; Bruinvels, A.; Hibert, M. Three-dimensional models of neurotransmitter G-binding protein coupled receptors. *Mol. Pharmacol.* **1991**, *40*, 8–15.
(6) Hancox, J. C.; McPate, M. J.; Harchi, A. E.; Zhang, Y. The hERG potassium channel and hERG screening for drug-induced torsades de pointes. *Pharmacol. Ther.* **2008**, *119*, 118–132. Redfern, W. S.; Carlsson, L.; Davis, A. S.; Lynch, W. G.; MacKenzie, I.; Palethorpe, S.; Siegl, P. K.; Strang, I.; Sullivan, A. T.; Wallis, R.; Camm, A. J.; Hammond, T. G. Relationships between preclinical cardiac electrophysiology, clinical QT interval prolongation and torsade de pointes for a broad range of drugs: evidence for a provisional safety margin in drug development. *Cardiovasc. Res.* **2003**, *58*, 32–45.
(7) Reasor, M. J.; Hatings, K. L.; Ulrich, R. G. Drug-induced phospholipidosis: issues and future directions. *Expert Opin. Drug Saf.* **2006**, *5*, 567–583.
(8) Horchler, C. L.; McCauley, J. P., Jr.; Hall, J. E.; Snyder, D. H.; Moore, W. C.; Hudzik, T. J.; Chapdelaine, M. J. Synthesis of novel quinolone and quinoline-2-carboxylic acid (4-morpholin-4-yl-phenyl)amides: a late-stage diversification approach to potent 5-HT_{1B} antagonists. *Bioorg. Med. Chem.* **2007**, *15*, 939–950.
(9) Bernstein, P.; Hill, D.; Nugiel, D.; Pierson, E.; Shenvi, A.; Jacobs, R. Chroman Compounds as 5-HT1B Receptor Antagonists, Their Preparation, Pharmaceutical Compositions, and Use in Therapy. PCT Int. Appl. WO 2007053095, **2007**.
(10) Information on this chroman was presented previously: Bernstein, P. R. Challenge of CNS Drug Discovery. Presented at the 235th National Meeting of the American Chemical Society, New Orleans, LA, Apr 6−10, **2008**; MEDI-143.
(11) Shenvi, A. Manuscript detailing the SAR of chroman and chromenone 5-HT_{1B} ligands is in preparation.
(12) Damewood, J. R.; Lerman, C. L. Flexible Ligand Alignment Protocols and Their Use in de Novo Design. Presented at the 234th National Meeting of the American Chemical Society, Boston, MA, Aug 19−23, **2007**; CINF-34. NovoFLAP is a proprietary computer-aided de novo tool that uses an evolutionary algorithm (EA-Inventor is available from Tripos International, 1699 South Hanley Rd, St. Louis, MO 63144) and a scoring function based on shape and pharmacophoric features.
(13) Sawyer, J. S.; Beight, D. W.; Britt, K. S.; Anderson, B. D.; Campbell, R. M.; Goodson, T.; Herron, D. K.; Li, H. Y.; McMillen, W. T.; Mort, N.; Parsons, S.; Smith, E. C.; Wagner, J. R.; Yan, L.; Zhang, F.; Yingling, J. M. Synthesis and activity of new aryl- and heteroaryl-substituted 5,6-dihydro-4*H*-pyrrolo[1,2-*b*]pyrazole inhibitors of the transforming growth factor-beta type I receptor kinase domain. *Bioorg. Med. Chem. Lett.* **2004**, *14*, 3581–3584.
(14) Suzuki, A. Synthetic studies via the cross-coupling reaction of organoboron derivatives with organic halides. *Pure Appl. Chem.* **1991**, *63*, 419–422.
(15) Robinson, G. E.; Cunningham, O. R.; Dekhane, M.; McManus, J. C.; O'Kearney-McMullan, A.; Mirajkar, A. M.; Mishra, V.; Norton, A. K.; Venugopalan, B.; Williams, E. G. Successful development and scale-up of a palladium-catalyzed amination process in the manufacture of ZM549865. *Org. Process Res. Dev.* **2004**, *8* (6), 925–930.
(16) For references and instrument applications, see www.thalesnano.com.
(17) This compound was resolved by chiral chromatography. Both enantiomers are partial agonists.
(18) Moderate human cLint (60 (μL/min)/mg) and an efflux ratio of 5.9 (B:A/A:B ratio in MDR1 transfected cells is described in the following: Hochman, J. H.; Pudvah, N.; Qiu, J.; Yamazaki, M.; Tang, C.; Lin, J.; Prueksaritanont, T. Interactions of human P-glycoprotein with simvastatin, simvastatin acid, and atorvastatin. *Pharm. Res.* **2004**, *21*, 1686–1691.
(19) Unpublished results. A variety of receptors that might have interfered with the in vivo experiments were specifically targeted. For binding assay information and values for standard reference compounds, see http://discovery.mdsps.com/Catalog/.
(20) Hatcher, J. P.; Slade, R. C.; Hagan, J. J. 5-HT_{1D} receptors mediate SKF 99101H-induced hypothermia in the guinea pig. *J. Psychopharmacol.* **1995**, *9*, 234–241.
(21) Hagan, J. J.; Slade, P. D.; Gaster, L.; Jeffrey, P.; Hatcher, J. P.; Middlemiss, D. N. Stimulation of 5-HT_{1B} receptors causes hypothermia in the guinea pig. *Eur. J. Pharmacol.* **1997**, *331*, 169–174.
(22) Bridgland-Taylor, M. H.; Hargreaves, A. C.; Easter, A.; Orme, A.; Henthorn, D. C.; Ding, M.; Davis, A. M.; Small, B. G.; Heapy, C. G.; Abi-Gerges, N.; Persson, F.; Jacobson, I.; Sullivan, M.; Albertson, N.; Hammond, T. G.; Sullivan, E.; Valentin, J.-P.; Pollard, C. E. Optimisation and validation of a medium-throughput electrophysiology-based hERG assay using IonWorks HT. *J. Pharmacol. Toxicol.* **2006**, *54*, 189–199.
(23) Morelli, J. K.; Buehrle, M.; Pognan, F.; Barone, L. R.; Fieles, W.; Ciaccio, P. J. Validation of an in vitro screen for phospholipidosis using a high-content biology platform. *Cell Biol. Toxicol.* **2006**, *22*, 15–27.
(24) In vivo pharmacology: Hudzik, T.; Smolka, J; Litwin, L.; Porrey, T.; Pierson, E. In vivo pharmacology of AZD1134, a novel 5-HT1B antagonist. *Eur. Neuropsychopharmacol.* **2003**, *13* (Suppl. 4), S181–S182. Process Chemistry (as M549865): Robinson, G. E.; Cunningham, O. R.; Dekhane, M.; McManus, J. C.; O'Kearney-McMullan, A.; Mirajkar, A. M.; Vikas Mishra; Norton, A. K.; Venugopalan, B.; Williams, E. G. Successful development and scale-up of a palladium-catalysed amination process in the manufacture of ZM549865. *Org. Process Res. Dev.* **2004**, *8*, 925–930. Development status: http://integrity.prous.com, entry no. 323892 .